

Structural study of amorphous selenium by *in situ* EXAFS: Observation of photoinduced bond alternation

Alexander V. Kolobov*

Joint Research Center for Atom Technology—National Institute for Advanced Interdisciplinary Research, 1-1-4, Higashi, Tsukuba, Ibaraki 305, Japan

Hiroyuki Oyanagi

Electrotechnical Laboratory, 1-1-4, Umezono, Tsukuba, Ibaraki 305, Japan

Kazunobu Tanaka

Joint Research Center for Atom Technology—National Institute for Advanced Interdisciplinary Research 1-1-4, Higashi, Tsukuba, Ibaraki 305, Japan

Keiji Tanaka

Department of Applied Physics, Faculty of Engineering, Hokkaido University, Sapporo 060, Japan

(Received 8 July 1996)

Photostructural change in amorphous selenium has been studied *in situ* by extended x-ray-absorption fine structure at 30 K. The essential features of the amorphous state are in agreement with the previous reports; the average bond length is shortened and the second-nearest-neighbor peak is smeared out, suggesting strengthening of intrachain and weakening of interchain interactions. In amorphous selenium, however, the coordination number is shown to be higher than 2 (~ 2.2) which is attributed to the presence of static threefold-coordinated sites in concentration about 20%. For these samples, we observe light-induced increase of the average coordination number (by $\sim 5\%$) and disorder while the bond length remains unchanged. This change is ascribed to the local formation of additional dynamical threefold-coordinated sites which increases structural disorder. Light-induced change of the coordination is *transient*: the initial coordination is restored after switching off the light, while the light-induced structural disorder remains. A microscopic mechanism of the light-induced structural change is proposed based on these experimental data. [S0163-1829(97)02602-7]

I. INTRODUCTION

Reversible photostructural changes in annealed thin films and melt-quenched bulk chalcogenide glasses^{1,2} have been the subject of numerous investigations but the microscopic mechanism of such changes still remains unclear. (See Ref. 3 for a recent review.) After direct proof of the changes in the structure evidenced by x-ray diffraction,⁴ various structural techniques such as IR, Raman, and extended x-ray-absorption fine structure (EXAFS) were used to study these changes.^{5–8} These measurements clearly demonstrated the irreversible changes in the structure of as-evaporated thin films under light irradiation and/or annealing which were attributed to polymerization of as-prepared films having molecular structures, but the reversible changes, which are most interesting from the fundamental point of view, were difficult to detect. A slight reversible change in the Raman spectra of annealed and illuminated As_2S_3 film was attributed to creation of a small number (about 6%) of “wrong” As-As bonds after illumination.⁶ EXAFS studies performed by various groups confirmed the formation of like-atom bonds on illumination of As_2S_3 glass (a somewhat smaller change of about 1%).^{7,8} At the same time, a change in the bond angle subtended at sulphur atoms was detected, accompanied by a simultaneous change in the dihedral angle between the adjacent AsS_3 pyramids.⁷ A similar change in the chalcogen bond angle was reported for another representative of arsenic

chalcogenides— $\text{As}_{50}\text{Se}_{50}$.⁹ X-ray photoemission spectroscopy studies performed for this glass revealed that a reversible change occurs in the density of states in the valence band on illumination and subsequent annealing.¹⁰

The formation of As-As bonds alone cannot explain the photodarkening, since in bulk As-S glasses any deviation from stoichiometry (the formation of As-As bonds, implying the formation of an equal number of S-S bonds, means local deviation of composition from stoichiometry) results in an increase of the forbidden gap¹¹ in contrast to experimental results where a decrease in the gap is observed as a result of light irradiation.³

It seems more likely that changes in the position of chalcogen atoms are responsible for the photodarkening. This conclusion comes from the fact that the top of the valence band is formed by nonbonding orbitals of chalcogen atoms and a change in mutual positions of chalcogen atoms, resulting in the change in the interaction between the lone-pair electrons, should cause a change in the forbidden gap. This argument is also supported by the observation that the value of a shift of the top of the valence band on illumination (~ 0.2 eV) is exactly the same as the (total) decrease in the optical gap.¹⁰ Correlations between the formation of “wrong” bonds and displacements of chalcogen atoms were recently shown.¹²

The interpretation of previous EXAFS data is not straightforward. Firstly, the chalcogenides studied were mostly bi-

nary glasses (with the exception of Ref. 13, where EXAFS of elemental selenium was reported) which made analysis of the data complicated. Elemental chalcogens, such as sulphur or selenium, which also exhibit reversible photodarkening,^{14,15} have basically not been studied, mainly because photo-induced changes in elemental chalcogens can only be realized at low temperature. Annealing the samples at room temperature results in a complete recovery of their initial parameters. The only reported EXAFS work on amorphous selenium¹³ (*a*-Se) evidenced that disorder in the material increases upon light irradiation.

Secondly, all previous measurements were performed *ex situ*, i.e., only annealed films and irradiated films were studied but a film kept *under* light irradiation *during* the measurement has never been studied. As a result, information about the excited state of the semiconductor and hence about the mechanism of the structural change was missing. It is therefore interesting to perform structural studies of light-induced changes in *a*-Se including investigation of the structure of the material kept under light excitation. EXAFS study of *a*-Se is also interesting since, despite previous efforts,^{16,17} the structure of *a*-Se is still not understood completely.

We have performed an *in situ* EXAFS study of photostructural changes in *a*-Se at 30 K and have observed pronounced changes in the first-coordination sphere.¹⁸ In this paper, the results of detailed analysis of EXAFS are discussed. First, the local structure of *a*-Se at low temperature is described with an emphasis on the average coordination number which measures the fraction of intrinsic over- or undercoordinated defect sites. The effect of photoexcitation at low temperature is then discussed providing the direct evidence for the dynamical bond formation.

II. EXPERIMENTAL

Our *a*-Se samples were thin films (0.1–0.3 μm thick) prepared by thermal evaporation of bulk selenium onto silica glass and aluminum-foil substrates. In order to anneal the films, they were kept at room temperature for at least 48 h before the measurements [the glass-transition temperature of selenium is about 30 °C (Ref. 11)].

The measurements were performed at BL 13B station at the Photon Factory¹⁹ using a 27-pole wiggler magnet inserted in a 2.5 GeV storage ring. We have chosen a fluorescence mode because of the fact that the samples with thicknesses smaller than the band-gap light penetration depth should be probed. Either arrays of 19-element high-purity Ge solid-state detectors²⁰ or 9 NaI(Tl) scintillation counters²¹ were used to detect the fluorescence. EXAFS spectra with good signal-to-noise ratio were obtained for thin films with 1000 Å thickness. A film of crystallized selenium (*c*-Se) with trigonal phase of a similar thickness was used as a standard to obtain experimental phase-shift function for the Se-Se pair.

Combination of high brilliance photon source and a densely packed detector array allowed us to improve the efficiency of fluorescence excitation and detection by two orders of magnitude. A directly water-cooled Si(111) double-crystal monochromator²² provided a stable and intense x-ray beam with an energy resolution of ~ 2 eV at 9 keV. High precision was achieved by *in situ* monitoring of the fluores-

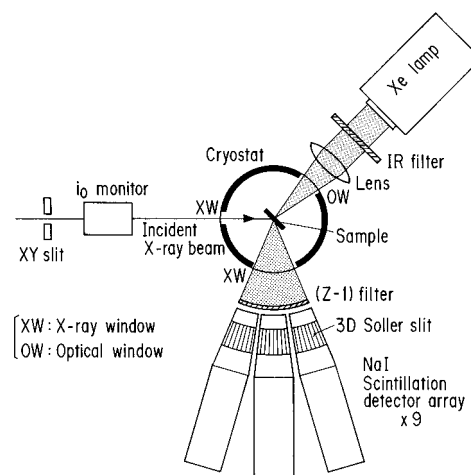


FIG. 1. Schematic diagram of the experimental setup.

cence monitoring the same region of uniform (evaporated film) sample at low temperature maintained within ± 0.1 K.

We have estimated possible uncertainties in the obtained values caused by the nonsystematic noise, i.e., photon counting statistics and electronic noise. Although it is difficult to estimate the systematic noise, we believe that the dominant source of error in our *in situ* experiments is beam instability since the effect of inhomogeneity in sample thickness is not present. We followed the recommended procedure²³ and measured several independent scans consecutively for a film of *crystalline* selenium which does not undergo structural transformations. The scatter in the data never exceeded $\pm 0.5\%$, which clearly demonstrates that *in situ* measurements under these conditions allowed us to achieve the accuracy in a relative change in coordination number and mean-square relative displacement (MSRD) within $\pm 1\%$ (compared to $\pm 20\%$ for conventional *ex situ* EXAFS).

The sample was mounted on an aluminum holder in an evacuated cryostat equipped with windows (kapton) for incident and fluorescent x-ray beams as well as an optical window (Mylar) for *in situ* light irradiation. A 500 W Xenon lamp with an IR-cutoff filter was used as an excitation source. The light was focused onto a 15 mm diameter spot for which the light intensity on the surface of the sample varied from 50 to 250 mW/cm^2 . A closed-cycle He refrigerator with a cooling power of ~ 9 W at 20 K was used. A schematic diagram of the experimental setup is illustrated by Fig. 1.

Se *K*-edge EXAFS spectra of *a*-Se and *c*-Se were measured in the temperature range from 15 to 300 K. The procedure for the study of photostructural changes was the following. After cooling the sample down to 30 K, the EXAFS spectrum of the starting (annealed) film was measured. After that the sample was irradiated in the cryostat for 1.5 to 7 h and an EXAFS spectrum of the photoexcited film *kept under light irradiation* was measured. Immediately after that, the Xenon lamp was switched off and the EXAFS spectrum of the irradiated sample but, *no longer kept under light irradiation*, was measured. In order to check reversibility, the irradiated sample was heated up to 300 K and kept at this temperature for 2 h which is sufficient to remove photodarkening¹⁴ and then cooled down to 30 K where the

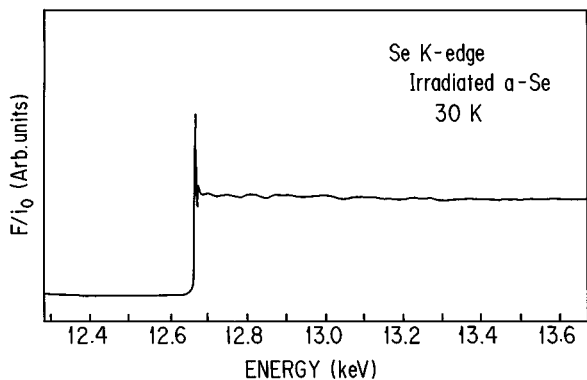


FIG. 2. Se K -edge fluorescence yield spectrum for amorphous selenium (a -Se) using an array of 9 NaI(Tl) scintillation counters and a 27-pole wiggler at the Photon Factory. The spectrum was taken at 30 K after illumination.

EXAFS spectrum was measured again. The whole procedure was repeated for several sets of samples.

III. RESULTS

A. a -Se versus c -Se

Figure 2 shows the raw Se $K\alpha$ fluorescence yield normalized by the incident beam intensity i_0 for an a -Se film taken at 30 K. In Fig. 3, the Se K -EXAFS oscillations are shown as a function of the photoelectron wave number k for a -Se and c -Se after subtraction of smooth backgrounds due to the atomic absorption, from the fluorescence yield spectra. The background function given as a combination of the third- and fourth-order polynomials, with tabulated coefficients²⁴ (Vic-

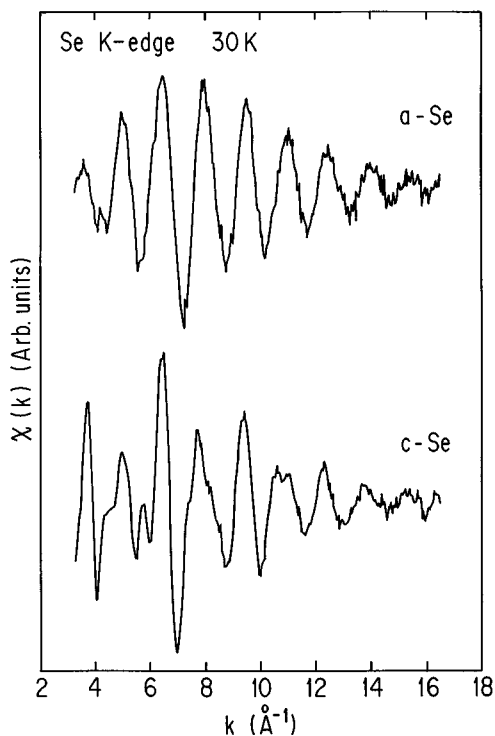


FIG. 3. Se K -EXAFS oscillations for amorphous selenium (a -Se, top) and crystalline selenium (c -Se, bottom) plotted as a function of photoelectron wave number k .

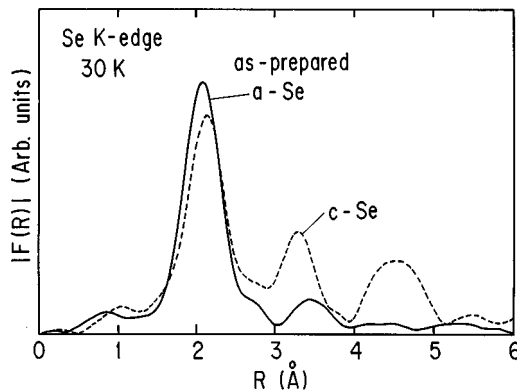


FIG. 4. Magnitude of Fourier transform of the Se K -EXAFS oscillations multiplied by k for as-prepared a -Se (solid line) and c -Se (dashed line) as a reference material to obtain the experimental Se-Se phase-shift function.

tooren Function) smoothly interpolates EXAFS oscillations. The cubic spline function was normalized to the edge jump and subtracted from the fluorescence yield spectrum. Because of rather high signal- (fluorescence) to-noise (scattering) ratio and a high fluorescence yield ($>10^6$ cps), high-quality data were collected in 50 min using NaI(Tl) scintillation counters and in 2 h using solid-state detector arrays.

The EXAFS oscillations multiplied by k [$k\chi(k)$] were Fourier transformed using the region extending from 4.5 to 15 \AA^{-1} . Typical results for the magnitude of Fourier transforms for c -Se and as-prepared a -Se films are shown in Fig.

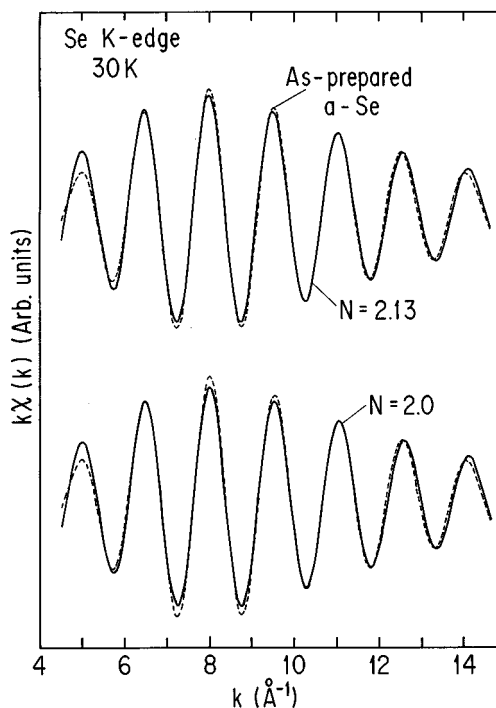


FIG. 5. Fourier-filtered first-shell Se K -EXAFS oscillations for as-prepared a -Se (solid line) and the results of a least-squares curve fitting (dashed line). The results of curve fit with a fixed coordination number (below) and optimized coordination number (above) are indicated.

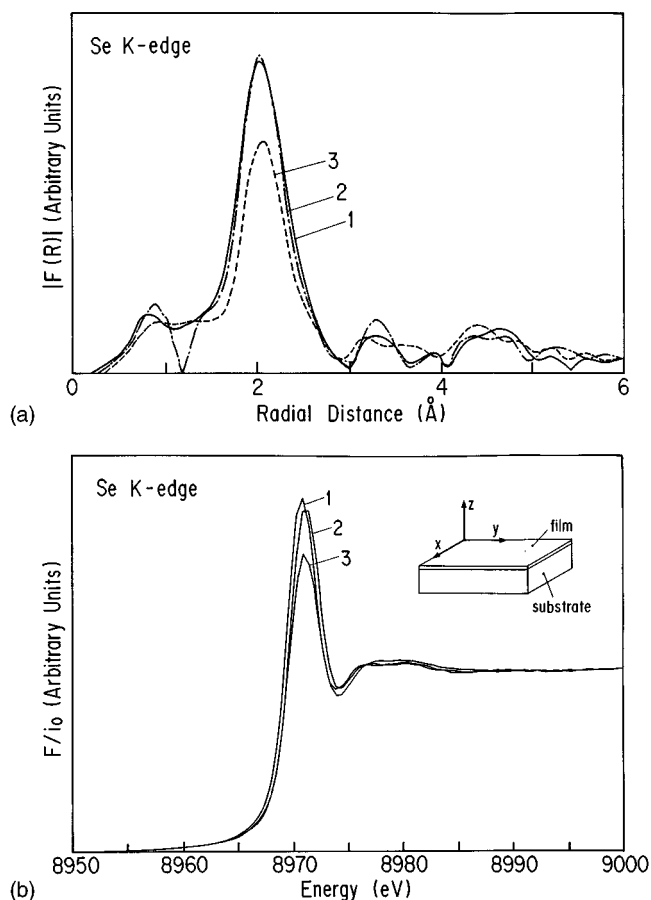


FIG. 6. X-ray-absorption near-edge structure (a) and Fourier-transformed EXAFS (b) spectra of polycrystalline *c*-Se film oriented at different angles with respect to electrical vector \mathbf{E} of x-rays. 1: $\mathbf{E}||x$, 2: $\mathbf{E}||y$, and 3: $\mathbf{E}||z$.

4. The prominent peaks observed at ~ 2 Å for *a*-Se and *c*-Se are due to the first-nearest selenium atoms. The peak positions are shifted to smaller r because of neglect of the phase-shift function. The second- and third-nearest peaks are well resolved for *c*-Se at ~ 3.3 and ~ 4.5 Å, respectively. For *a*-Se, the second peak has a smaller magnitude and is shifted to larger r broadening the distribution, while the third peak is smeared out. One can see that the height of the first peak for *a*-Se is greater than that for *c*-Se in agreement with Ref. 25 and in contrast to other amorphous semiconductors. Such a change of the short-range order in the amorphous state is unusual among semiconductors such as *a*-Si or *a*-Ge where the nearest-neighbor peak slightly decreases going from the crystalline to the amorphous state as a result of structural disorder.^{26–28}

For the quantitative EXAFS data analysis, the Fourier-transformed data were filtered in order to extract the contribution of the first-nearest neighbors, and back-Fourier transformed into k space. The filtered data for the first shell together with the results of least-squares curve fitting based on a single scattering theory are shown in Fig. 5 for *a*-Se. The fitting, based on a single scattering theory,²⁹ was performed using two different approaches in order to minimize the effect of the correlation between the coordination number and the disorder parameter. In the first approach, the coordination number was kept constant and only the change in the

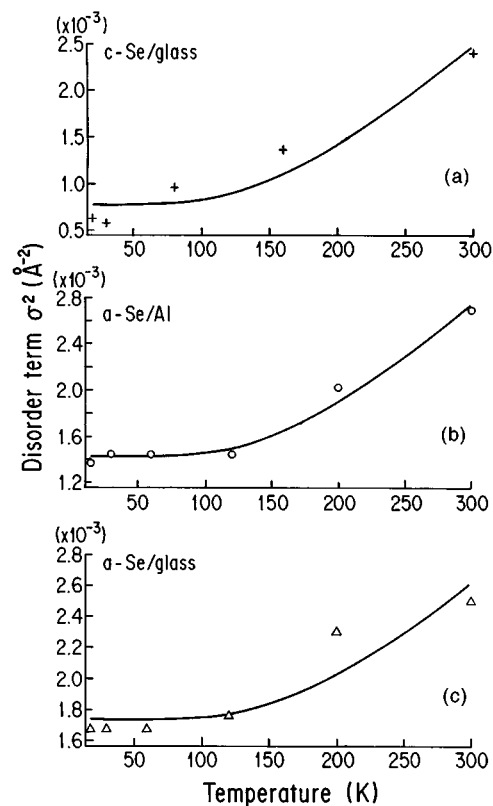


FIG. 7. Temperature dependence of MSR for *c*-Se (a) and *a*-Se deposited onto aluminum (b) and silica glass (c) substrates. Solid lines represent theoretical fit using the Einstein model.

bond length and the mean-square relative displacement (MSRD) σ^2 were allowed. In the second approach, all parameters were allowed to vary. This is equivalent to the correlation analysis where the contour map with the two parameters is obtained. We note that the curve fit results were also confirmed by a model-independent ratio method³⁰ on the basis of the fact that the bond length was unchanged between the two phases.

The curve-fitting analysis in the case of an *a*-Se film gives the coordination number close to 2.15. The bond length in the crystalline film is 2.36 ± 0.1 Å and that in an amorphous film is 2.32 ± 0.01 Å. These values are in agreement with the data obtained by other groups.^{31,32}

Oriented *c*-Se film is expected to be strongly anisotropic because of its linear chain structure. This could result in the modulated coordination number for *a*-Se because of polarization factor $3 \cos^2\theta$, where θ denotes the angle between an electrical vector \mathbf{E} and the Se-Se bond. In order to exclude this possibility, we have measured the orientational dependence of EXAFS and XANES for the *c*-Se film at room temperature for different orientations of the sample around the vertical axis. The results of this measurement is shown in Fig. 6. It can be seen that the (polycrystalline) Se film is indeed *anisotropic*. The difference in the coordination numbers obtained for different sample orientations could be about 20%. This anisotropy of the reference sample was taken into account (by averaging over various directions) when the coordination number for *a*-Se was determined.

Figure 7 shows the temperature dependence of MSR for *c*-Se and *a*-Se deposited onto silica glass and aluminum sub-

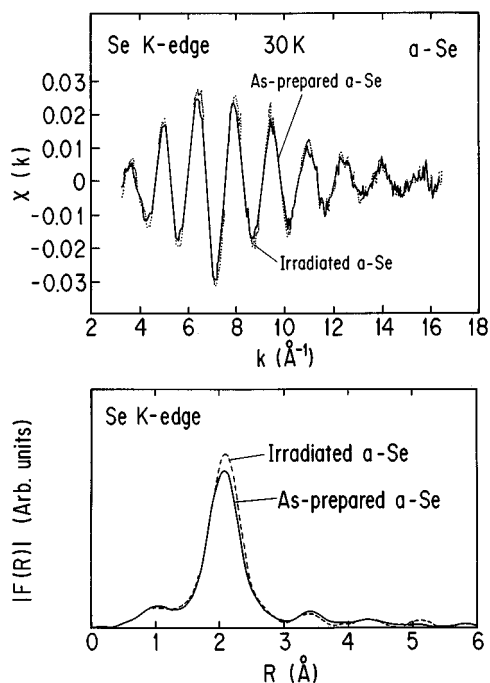


FIG. 8. Raw EXAFS (top) and magnitude of Fourier transform (bottom) of the Se K -EXAFS oscillations multiplied by k for virgin a -Se film (solid line) and irradiated film under light excitation (dashed line).

strates. One can see that MSRDR increases with temperature for both c -Se and a -Se. At lower temperatures MSRDR is not dependent on temperature due to static disorder.

B. Light-induced changes in a -Se

Although the EXAFS technique is a local probe on a particular species of atom, the information is averaged over all sites. Thus in general, it is difficult to observe the spatially limited light-induced effect as a distinct variation in the magnitude of Fourier transform. However, using *in situ* measurements with optimized excitation light intensity and exposure time, we were able to detect the photostructural change. Raw EXAFS spectra of the virgin and photoexcited a -Se films as well as the results of Fourier transform are shown in Fig. 8. The least-squares curve fit analysis based on the two approaches described in the previous section confirmed the structural change in terms of both coordination number and disorder parameter: in all measurements, the R factor, defined as a sum-up of the mean-square differences between the experimental data and simulated curve, is minimized when all parameters were allowed to vary. The result was independent on choice of theoretical amplitudes if they are properly normalized to reproduce the reference (c -Se) EXAFS amplitude.

In Fig. 9, variations in the bond length, normalized coordination number, and disorder parameter (MSRD) associated with sequences of sample treatment, i.e., as-prepared, under illumination, after illumination and after annealing, are summarized. One can see that the bond length is essentially independent on the irradiation (which justifies the use of the ratio method), although a slight substrate dependence is observed possibly due to the effect of strain. The coordination

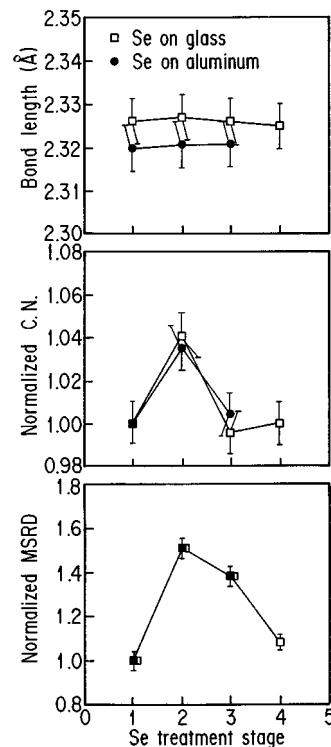


FIG. 9. Results of a least-squares curve fit analysis of the Se K -EXAFS data for a -Se plotted against the treatment stage (1: as-prepared, 2: under illumination, 3: after illumination and 4: after heat treatment at 300 K). The figures show the Se-Se bond length for a -Se deposited on silica glass and aluminum substrates (top), the normalized coordination number (middle) and the normalized mean-square relative displacement (bottom). The normalization was performed to the data for the initial state.

number increases reversibly in the sample kept under irradiation by about 4%, which is significantly larger than the experimental uncertainty in our *in situ* experiment. The value varied from 2 to 7% depending on light intensity and exposure time which is discussed elsewhere.³³ Associated with the change in coordination, the MSRDR also increases under light irradiation. After illumination, the local change of coordination disappears, while the light-enhanced structural disorder remains. Although the magnitude of structural disorder varies from sample to sample, the normalized change in both coordination number and MSRDR gave similar results. Thus we conclude that this change of structure, averaged over all sites, indicates a locally increased coordination number such as threefold-coordinated sites. Annealing of the irradiated sample at 300 K results in complete recovery of the initial values for both the coordination number and the disorder parameter.

We have analyzed the coordination number for a -Se as-prepared, under illumination and after annealing. The results of the curve-fit analysis systematically varying the value of fixed coordination number around the value obtained by all-parameter fit are shown in Fig. 10. The change of coordination as a result of various stages of illumination is clearly demonstrated. The ratio method³⁰ also confirmed that both coordination number and disorder increase as a result of light irradiation.

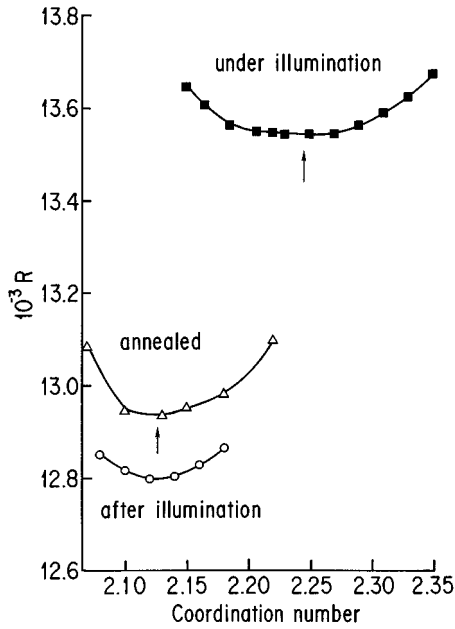


FIG. 10. R factor is plotted as a function of bond length with fixed coordination number for least-squares curve fit around the value obtained from the all-parameter fit. An increase in the coordination number in the excited state is clearly seen.

We would like to stress once more that the error bars, which are usually about $\pm 20\%$ for absolute coordination number in conventional EXAFS, are significantly decreased in our *in situ* study since we always probe the *same* area. In our case, the error bars for the relative change in coordination are smaller than 1% and this substantial decrease is caused by excluding the systematic error due to the fluctuation of beam position which is the main source of error in coordination number. The remaining factor of systematic noise, the fluctuation of the beam intensity in the incident beam, was minimized by the inspection of the quality for repeated scans. Our independent measurements over several sets of samples gave very good repeatability of the observed changes.

IV. DISCUSSION

A. *a*-Se versus *c*-Se

The observation of a greater coordination number than two in *a*-Se is ascribed to the threefold-coordinated sites. The possibility of polarization effect (orientation of linear chains) is ruled out as discussed in the previous section. Previous models^{34–36} assumed that uncharged defects, expressed by two neutral dangling bonds, produce pairs of threefold-coordinated sites and singly coordinated charged sites called valence-alternation pairs (VAP):



Although the VAP model has attracted much attention in relation to photoinduced effects in chalcogenide glasses,³⁴ such a model is not consistent with the experimental observation, i.e., the average coordination number (2.0) should be preserved since the charged sites are equal in number. Recent molecular-dynamics calculations found that the average co-

ordination number in *a*-Se is 2.17 at 350 K.³² Taking the experimental error in determining the absolute coordination number into account, this result is in good agreement with the present observation (2.13).

The results of curve-fit analysis using different theoretical amplitude functions^{37,38} showed that the coordination number is independent of the choice of theoretical backscattering amplitude, while the MSRD values are dependent on $|f_j(k, \pi)|$. The use of the parameters of Teo and Lee³⁷ gave the MSRD values of about 0.001 29 and 0.001 76 \AA^2 for annealed and irradiated films, respectively, while the use of the FEFF (Ref. 38) gave a much smaller MSRD value of less than 0.000 12 \AA^2 for annealed and 0.000 36 \AA^2 for irradiated films. It is found that the normalized coordination number, defined as a ratio of coordination number between the measurements before and after irradiation, gives a good convergence, however.

The bond length shortening in the amorphous state is unusual since the unharmonicity of the two-body potential should increase the bond length as observed for Ge (Ref. 26) and Si.²⁷ However, this is not the case where the short-range order changes. In selenium, the *interchain* distance is close to the *intrachain* second-nearest distance.¹⁶ The structural disorder in the amorphous state relaxes the folded spiral chain. As a result of decreased Coulomb repulsion, this would increase the overlap integral, or the bond charge, shortening the bond length. Similar arguments were made to explain a decrease in the bond length of selenium chains confined in mordenite channels.³⁹

The rearrangement of *interchain* interaction was also observed as a shift of the second-nearest peak away from the first-nearest neighbor peak. The helical chain structure in trigonal *c*-Se originates from minimization of the intra- and *interchain* repulsive interactions. The essential feature of *a*-Se is therefore the strengthened *intrachain* interaction and weakened *interchain* interaction. An increase of the second-nearest distance in the amorphous state may reflect the enhancement of the *p*-like character of the Se-Se bond, which is stabilized by maximizing the distance between the second-nearest neighbors. Such a trend is demonstrated in the magnitude of the Fourier transform in Fig. 3, which is consistent with an increase of the band gap associated with the intensified homopolar bond charge.^{40,41}

We now turn our attention to the temperature dependence of the MSRD in *c*-Se and *a*-Se. In *c*-Se, the MSRD increases with T over a wide range since the thermal vibration term dominates. In the case of *a*-Se, the temperature variation is only observed for $T > 150$ K. At lower temperatures, MSRD is constant implying that the static disorder dominates at those temperatures. Application of a simple formula based on the Einstein model⁴²

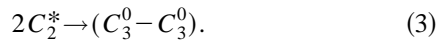
$$\sigma^2 = C_1 + [h/\mu\omega_E] \coth(h\omega_E/kT), \quad (2)$$

where C_1 characterizes a degree of static disorder, μ is the atom mass, and ω_E is a characteristic frequency, allows us to estimate the value ω_E , which is a measure of the bond strength. ω_E equals $6.7 \times 10^{13} \text{ s}^{-1}$ for *c*-Se. Application of the same formula to *a*-Se (with larger error bars because the number of data points is very limited) gives a rough estimate of ω_E to be $7.3 \times 10^{13} \text{ s}^{-1}$ for the *a*-Se film on an aluminum

substrate and $8.2 \times 10^{13} \text{ s}^{-1}$ for *a*-Se on a silica glass substrate. The fact that ω_E is larger for *a*-Se implies that the Se-Se bond is stronger in the disordered state in agreement with the conclusion obtained from the bond length shortening in *a*-Se. An increase in ω_E for the *a*-Se film deposited onto a glass substrate is possibly caused by extra disorder. The internal strain caused by different thermal-expansion coefficients of *a*-Se and silica glass would increase the bond stretching near the interface. The effect of strain also results in the slightly longer bond length in the film in contact with the silica glass substrate.

B. Light-induced changes in *a*-Se

The light-induced increase in the coordination number is interpreted as indicating the formation of higher-than-twofold-coordinated sites. Under light irradiation, electrons from the top of the valence band, formed by lone-pair (LP) electrons, are excited into the conduction band leaving one electron in the former LP orbital. Provided the distance between such excited atoms is close to the covalent bond length and the spins have opposite directions, additional covalent bonds can be dynamically formed between excited atoms, making a part of selenium atoms threefold coordinated. This can happen in the excited state since a large number of photoexcited carriers screen the positive charge centered on threefold-coordinated atoms. The process of dynamical bond formation is expressed by the following formula where C_2^* denotes twofold excited lone-pair states:



The formation of these new *interchain* bonds is expected to introduce a local distortion around the threefold-coordinated sites, which would result in an increase in the MSRD. The formation of dynamical bonds would also cause the displacement of near-neighbor atoms.

The incident photon flux in our experiment was about $10^{18} \text{ photons/cm}^2 \text{ s}$, while the absorption coefficient was of the order of 10^4 cm^{-1} . Then for a 1000 Å film, the number of absorbed photons is about $10^{17} \text{ photons/cm}^2 \text{ s}$ or 1 photon/atom s. A rough estimate of carrier lifetime in selenium in our experimental conditions, using the lifetime temperature dependence in a rather limited temperature range for *a*-As₂Se₃,⁴³ and room-temperature values of lifetime in *a*-Se,⁴⁴ gives a typical lifetime value in the range from a millisecond to a second. Unfortunately, the lack of experimental data for carrier lifetime in *a*-Se at low temperatures does not allow us to make a better estimate. These two values result in the average concentration of light-excited atoms of the order of a few percent under our experimental conditions which is a reasonable concentration required by the suggested model.

After cessation of light irradiation, the photo-excited electrons recombine. However, since the formation of a third bond removes an electron from an LP orbital to a bonding orbital, a corresponding empty state is forced to move to an antibonding orbital and the recombination in the excited-state configuration is impossible as there is no empty state in the valence band. Bond breaking is a necessary process for the recombination. This process can proceed along three different pathways shown in Fig. 11. First, the newly formed

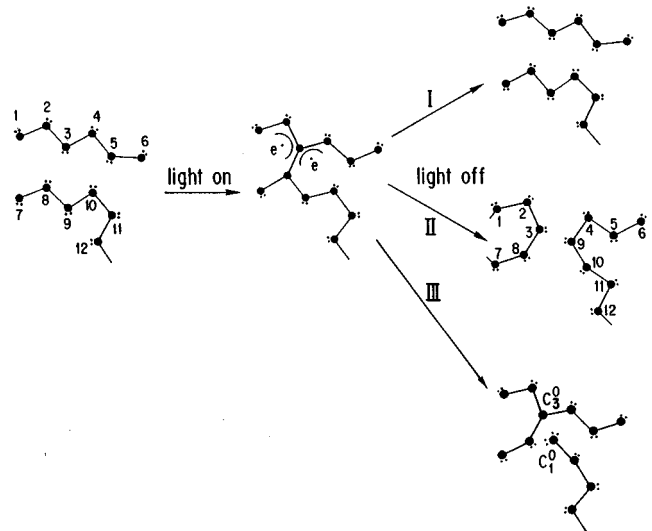


FIG. 11. A schematic diagram of the local structural change in selenium chains as a result of illumination and that after the illumination. Interchain bond formation under photoexcitation at low temperature forms the threefold-coordinated sites which increases the local distortion observed as the increase in the mean-square relative displacement. There could be different pathways of returning to the ground state. In path I, initial bonds are restored, while in path II, new bonds are formed between atoms belonging to different chains. In path III, pairs of threefold-coordinated sites and onefold-coordinated sites are formed. See text for details.

bonds may break after which the initial structure is restored (path I). Second, strained bonds in the vicinity of the newly formed bonds may be broken, e.g., as demonstrated by path II in Fig. 11, in which case the initial coordinating number is also restored. However, the system may not recover the original configuration with the minimum *local* energy which would introduce the additional disorder. And, finally, there is also possibility that a bond in the vicinity of the newly formed bond is broken resulting in the formation of a defect pair composed of a singly coordinated and triply coordinated selenium atoms, similar to a valence alternation pair (path III), where the initial average coordination number is also restored. The bond length difference for such singly and triply coordinated atoms should increase the MSRD also.

Although we cannot make a clear distinction between the two possibilities (path II and path III), the formation of As-As bonds in As₂S₃ on irradiation^{6,7} suggests that path II in Fig. 11 may be operative. On the other hand, results of light-induced electron-spin resonance (LESR) experiments for the same material⁴⁵ support the possibility indicated by path III. Most likely, the two paths coexist. Further studies are needed in order to elucidate which of them is dominant in each particular case. More recent results of LESR for *a*-Se (Ref. 46) indicate that path III is most likely to be the case, although the stable configuration is strongly dependent on temperature.

One could argue that an increase in the MSRD under light irradiation could be caused by thermal excitation. Although there may exist some heat-up of the sample, we believe that this is not a decisive factor due to the following arguments. First, we estimate that the temperature increase cannot be higher than a few degrees. Second, the effect is hardly de-

pendent on the substrate material (silica glass and aluminum), although heat dissipation conditions change drastically. And, third, the T dependence of the MSRD indicates that an increase in temperature up to 150 K does not lead to an increase in MSRD (see Fig. 7) and should not affect the coordination number.

A thin film of about $0.1 \mu\text{m}$ used in our experiment can easily be affected by the presence of strain since the substrate strongly influences the properties of chalcogenide films of much higher thicknesses.⁴⁷ A small difference in the Se-Se bond length in a -Se deposited onto silica glass and aluminum are most likely caused by a difference in the thermal-expansion coefficients of the two substrates; the film is more relaxed on aluminum since the thermal-expansion coefficient of aluminum is greater and closer to that of a -Se. The films deposited on silica is stretched giving a greater bond length as observed experimentally.

The observed formation of dynamical bonds in the photoexcited state, in which lone-pair electrons play a decisive role, allows one to understand why reversible photostructural changes can only be observed in amorphous chalcogenides and not in other amorphous semiconductors such as arsenic⁴⁸ or hydrogenated amorphous silicon.⁴⁹ Although an important role of lone-pair electrons for this process was recognized^{3,50} in previous papers, it was stated as a mere ‘‘hypothesis.’’³ The mechanism of the photostructural change suggested by the present results demonstrates that bond formation occurs first followed by bond breaking, in sharp contrast to the conventional understanding of the photostructural change which assumes bond breaking to be the initial process.^{3,51–53}

Very important is the observed similarity between the structure of a -Se in the photoexcited state and that of liquid selenium; thermal excitation and optical pumping lead to the same short-range order change. This similarity gives the clue to a more general understanding of the photostructural change as local athermal quasimelting at low temperature permitting a large degree of local lattice relaxation in the absence of steric hindrance. For example, this explains why the photoinduced fluidity⁵³ in a chalcogenide glass increases

at lower temperatures since the number of photoinduced defects increases as the temperature decreases.

V. CONCLUSION

The average coordination number of selenium in the amorphous state is about 2.2, which means that about 20% of selenium atoms are threefold coordinated. The observed change of bond length and mean-square relative displacement in the amorphous state is interpreted in terms of weakening of *interchain* interaction and strengthening of *intra-chain* interaction in the amorphous state.

We found that light illumination increases the average selenium coordination number, which suggests that about 5% of additional selenium atoms become threefold coordinated. This indicates that new interchain covalent bonds are formed *dynamically and locally* as a result of bond alternation during the irradiation. After cessation of light irradiation, the initial (average) number of twofold sites is restored. The dynamical bond alternation introduces additional structural disorder during the illumination which is quenched to static disorder at 30 K. It was found that annealing at room temperature leads to recovery of the initial structure. These results provide direct evidence for the dynamical structural change induced by bond alternation during photoexcitation. They also explain why reversible photostructural change can only be observed in amorphous chalcogenides.

ACKNOWLEDGMENTS

This work, partly supported by NEDO, was performed in the Joint Research Center for Atom Technology (JRCAT) under the joint research agreement between the National Institute for Advanced Interdisciplinary Research (NAIR) and the Angstrom Technology Partnership (ATP). The measurements were done at the Photon Factory as part of a research Project No. 95G026. A.V.K. and H.O. gratefully acknowledge a very useful discussion with Professor E. A. Stern and his comments on the estimation of the experimental uncertainties.

*On leave from A. F. Ioffe Physico-Technical Institute.

¹S. A. Keneman, Appl. Phys. Lett. **19**, 205 (1971).

²J. S. Berkes, S. W. Ing, and W. J. Hillegas, J. Appl. Phys. **42**, 4908 (1971).

³G. Pfeifer, M. A. Paesler, and S. C. Agarwal, J. Non-Cryst. Solids **114**, 130 (1989), and references therein.

⁴K. Tanaka, Appl. Phys. Lett. **26**, 243 (1975).

⁵D. J. Treacy, P. C. Taylor, and P. B. Klein, Solid State Commun. **32**, 423 (1978).

⁶M. Frumar, A. P. Firth, and A. E. Owen, Philos. Mag. B **50**, 463 (1984).

⁷C. Y. Yang, M. A. Paesler, and D. E. Sayers, Phys. Rev. B **36**, 9160 (1987).

⁸L. F. Gladden, S. R. Elliott, and G. N. Greaves, J. Non-Cryst. Solids **106**, 189 (1988).

⁹S. R. Elliott and A. V. Kolobov, Philos. Mag. B **61**, 853 (1990).

¹⁰A. V. Kolobov, Yu. P. Kostikov, S. S. Lantratova, and V. M. Lyubin, Sov. Phys. Solid State **33**, 444 (1991).

¹¹Z. U. Borisova, *Glassy Semiconductors* (Plenum, New York, 1981).

¹²A. V. Kolobov and G. J. Adriaenssens, Philos. Mag. B **71**, 1 (1995).

¹³Y. Katayama, M. Yao, Y. Ajiro, M. Inui, and H. Endo, J. Phys. Soc. Jpn. **58**, 1811 (1989).

¹⁴V. L. Averyanov, A. V. Kolobov, B. T. Kolomiets, and V. M. Lyubin, Phys. Status Solidi A **57**, 81 (1980).

¹⁵Ke Tanaka, Jpn. J. Appl. Phys. **25**, 779 (1986).

¹⁶P. Andonov, J. Non-Cryst. Solids **47**, 297 (1982).

¹⁷B. W. Corb, W. D. Wei, and B. L. Averbach, J. Non-Cryst. Solids **53**, 29 (1982).

¹⁸A. V. Kolobov, H. Oyanagi, K. Tanaka, and Ke Tanaka, J. Non-Cryst. Solids **198-200**, 709 (1996).

¹⁹H. Oyanagi, R. Shyoda, Y. Kuwahara, and K. Haga, J. Synch. Radiat. **2**, 99 (1995).

²⁰H. Oyanagi, M. Martini, M. Saito, and K. Haga (unpublished).

²¹H. Oyanagi, T. Matsushita, H. Tanoue, T. Ishiguro, and K. Kohra, Jpn. J. Appl. Phys. **24**, 610 (1985).

²²H. Oyanagi, K. Haga, and Y. Kuwahara, Rev. Sci. Instrum. **67**, 350 (1996).

²³F. W. Lytle, D. E. Sayers, and E. A. Stern, Physica B **158**, 702 (1989).

- ²⁴*International Tables for X-ray Crystallography* (Kynoch, Birmingham, 1962), Vol. III.
- ²⁵D. E. Sayers, in *Proceedings of the 7th International Conference on Amorphous and Liquid Semiconductors*, edited by W. E. Spear (University of Edinburgh, Edinburgh, 1977), p. 61.
- ²⁶M. Wakagi, M. Chigasaki, and M. Nomura, *J. Phys. Soc. Jpn.* **56**, 1765 (1987).
- ²⁷M. Wakagi, K. Ogata, and A. Nakano, *Phys. Rev. B* **50**, 10 666 (1994).
- ²⁸J. Freund, R. Ingalls, and E. D. Grozier, *J. Phys. Chem.* **94**, 1087 (1990).
- ²⁹E. A. Stern, *Phys. Rev. B* **10**, 3027 (1974).
- ³⁰E. A. Stern, D. E. Sayers, and F. W. Lytle, *Phys. Rev. B* **11**, 4836 (1975).
- ³¹N. F. Mott and E. A. Davis, *Electronic Processes in Non-Crystalline Materials*, 2nd ed. (Clarendon, Oxford, 1979), p. 518, and references therein.
- ³²D. Hohl and R. O. Jones, *Phys. Rev. B* **43**, 3856 (1991).
- ³³A. V. Kolobov, M. Kondo, H. Oyanagi, A. Matsuda, and K. Tanaka (unpublished).
- ³⁴R. A. Street and N. F. Mott, *Phys. Rev. Lett.* **35**, 1293 (1976).
- ³⁵M. Kastner, D. Adler, and H. Fritzsche, *Phys. Rev. Lett.* **37**, 1504 (1976).
- ³⁶D. Vanderbilt and J. D. Joannopoulos, *Phys. Rev. B* **22**, 2927 (1980).
- ³⁷B. K. Teo and P. A. Lee, *J. Am. Chem. Soc.* **101**, 2815 (1979).
- ³⁸A. G. McKale, B. Ww. Veal, A. P. Paulikas, S. K. Chan, and G. S. Knapp, *J. Am. Chem. Soc.* **110**, 3763 (1988).
- ³⁹K. Tamura, S. Hosokawa, H. Endo, S. Yamasaki, and H. Oyanagi, *J. Phys. Soc. Jpn.* **55**, 528 (1986).
- ⁴⁰L. Pauling, *The Nature of the Chemical Bond* (Cornell University Press, Ithaca, New York, 1960), Chap. 4.
- ⁴¹J. A. Van Vechten and J. C. Phillips, *Phys. Rev. B* **2**, 2160 (1970).
- ⁴²P. P. Loticci, G. Antonioli, and C. Razzetti, *Physica B* **158**, 517 (1989).
- ⁴³N. F. Mott and E. A. Davis, *Electronic Processes in Non-Crystalline Materials* (Ref. 31), p. 262.
- ⁴⁴M. D. Tabak and P. J. Warter, *Phys. Rev.* **173**, 899 (1968).
- ⁴⁵D. K. Biegelsen and R. A. Street, *Phys. Rev. Lett.* **44**, 803 (1980).
- ⁴⁶A. V. Kolobov, M. Kondo, H. Oyanagi, R. Durni, A. Matsuda, and K. Tanaka (unpublished).
- ⁴⁷A. V. Kolobov and S. R. Elliott, *Philos. Mag. B* **71**, 1 (1995).
- ⁴⁸E. Mytilineou, P. C. Taylor, and E. A. Davis, *Solid State Commun.* **35**, 497 (1980).
- ⁴⁹K. Tanaka, *J. Non-Cryst. Solids* **137&138**, 1 (1991).
- ⁵⁰A. V. Kolobov, K. Shimakawa, and S. R. Elliott, *Adv. Phys.* **44**, 475 (1995).
- ⁵¹V. L. Averyanov, A. V. Kolobov, B. T. Kolomiets, and V. M. Lyubin, *J. Non-Cryst. Solids* **45**, 343 (1981).
- ⁵²S. R. Elliott, *J. Non-Cryst. Solids* **81**, 71 (1986).
- ⁵³H. Hisakuni and K. Tanaka, *Science* **270**, 974 (1995).